Inferring the Individual Psychopathologic Deficits with Structural Connectivity in a Longitudinal Cohort of Schizophrenia

Yi Sun, Zhe Zhang, Ioannis Kakkos, George K. Matsopoulos, *Member, IEEE*, Jingjia Yuan, John Suckling, Luoyi Xu, Shuxia Cao, Wenjuan Chen, Xingyue Hu, Tao Li, Kang Sim, Peng Qi*, *Member, IEEE*, and Yu Sun*, *Senior Member, IEEE*

***Abstract*—The prediction of schizophrenia-related psychopathologic deficits is exceedingly important in the fields of psychiatry and clinical practice. However, objective association of the brain structure alterations to the illness clinical symptoms is challenging. Although, schizophrenia has been characterized as a brain dysconnectivity syndrome, evidence accounting for neuroanatomical network alterations remain scarce. Moreover, the absence of generalized connectome biomarkers for the assessment of illness progression further perplexes the prediction of long-term symptom severity. In this paper, a combination of individualized prediction models with quantitative graph theoretical analysis was adopted, providing a comprehensive appreciation of the extent to which the brain network properties are affected over time in schizophrenia. Specifically, Connectome-based Prediction Models were employed on Structural Connectivity (SC) features, efficiently capturing individual network-related differences, while identifying the anatomical connectivity disturbances contributing to the prediction of psychopathological deficits. Our results demonstrated distinctions among widespread cortical circuits responsible for different domains of symptoms, indicating the complex neural mechanisms underlying schizophrenia. Furthermore, the generated models were able to significantly predict changes of symptoms using SC features at follow-up, while the preserved SC features suggested an association with improved positive and overall symptoms. Moreover, cross-sectional significant deficits were observed in network efficiency and a progressive aberration of global integration in patients compared to healthy controls, representing a group-consensus pathological map, while supporting the dysconnectivity hypothesis.**

***Index Terms*—Schizophrenia, structural connectivity, longitudinal, connectome-based prediction model.**

This work was funded by the National Natural Science Foundation of China (81801785, 81801279, 82172056), by the Zhejiang Lab (2019KE0AD01, 2021KE0AB04), by the Zhejiang University Global Partnership Fund (100000-11320), by the National Key R&D Program of China (2018YFC1314200), National Healthcare Group (NHG 11003, 12003), and the A*STAR/Singapore Bioimaging Consortium (ASTAR/SBIC009/2006). (∗, *Corresponding author: Peng Qi, Yu Sun.*)

Yi Sun, L. Xu, S. Cao, W. Chen and X. Hu are with the Department of Neurology, Sir Run Run Shaw Hospital, Zhejiang University School of Medicine, Hangzhou 310020, Zhejiang, China.

Z. Zhang and J. Yuan are with the Key Laboratory for Biomedical Engineering of Ministry of Education of China, Department of Biomedical Engineering, Zhejiang University, Hangzhou 310007, Zhejiang, China.

I. Kakkos and G. K. Matsopoulos are with the School of Electrical and Computer Engineering, National Technical University of Athens, Athens 15780, Greece.

P. Qi is with the Department of Control Science and Engineering, College of Electronics and Information Engineering, Tongji University, Shanghai 200092, China (email: pqi@tongji.edu.cn).

J. Suckling is with Brain Mapping Unit, Department of Psychiatry, School of Clinical Medicine, Herchel Smith Building for Brain and Mind Sciences, University of Cambridge, Cambridge CB2 0SP, United Kingdom.

T. Li is with the Affiliated Mental Health Center & Hangzhou Seventh People's Hospital, Mental Health Center, Zhejiang University School of Medicine, Hangzhou 310013, Zhejiang, China.

K. Sim is with the Department of General Psychiatry, and the Department of Research, Institute of Mental Health, Singapore 539747, Singapore

Yu Sun is with the Department of Neurology, Sir Run Run Shaw Hospital, Zhejiang University School of Medicine, and also with the Key Laboratory for Biomedical Engineering of Ministry of Education of China, Zhejiang University, and also with Zhejiang Lab, Hangzhou 310027, Zhejiang, China (e-mail: yusun@zju.edu.cn).

I. Introduction

SCHIZOPHRENIA is a complex neuropsychiatric disorder with numerous symptoms and clinical manifestations [1], [2]. Since various causes have been linked to schizophrenia, no objective diagnostic criteria can be directly applied for severity/prognosis assessment, while the precise neural substrates underpinning its heterogeneous clinical aspects are yet to be achieved. To date, psychiatric research employs the Positive and Negative Syndrome Scale (PANSS) as the "gold standard" to estimate diagnostic and treatment efficacy as well as the symptom severity of schizophrenic patients [3]. As such, PANSS presents a stable factor structure with inter-rater reliability and a valid taxonomy of positive, negative and general psychopathology symptoms.

Establishing the association between the differences in clinical symptoms/cognitive states and the alterations in brain structure/function is a convergent research interest of modern psychiatry studies [4]. In addition, unlike prior assumptions that consider schizophrenia to be associated with specific brain region abnormality, recent evidence support that interaction deficits in the neural circuitry can efficiently model the underlying effects on the human brain [5], [6], [7], coinciding with the recent advent of human connectome studies [8]. On this premise, distortions in the White Matter (WM) could account for information transmission deficiency between the different brain areas [9]. However, only a few studies have examined the longitudinal effects on WM microstructure in schizophrenic patients [10], [11], with a particular focus on the assessment of pharmacological treatment response in the first episode patients [12]. In this regard, no study has investigated the feasibility of utilizing WM to predict clinical measures of illness progression, therefore providing no conclusive evi-

dence of long-term disorder-related WM alterations in chronic schizophrenia.

Another important limitation is that although previous studies have demonstrated that structural connectivity (SC) alterations are correlated with clinical symptoms [5], [7] and that resting-state functional connectivity predicts treatment responses [13] and clinical symptoms [4], no research works, have incorporated SC for psychopathological deficits prediction on the individual level. In this regard, the most frequently employed approaches assume between-group comparisons with a healthy cohort by correlating neuroimaging measures with clinical measures [14]. While these studies are valuable in terms of suggesting relevant disease indicators, case-control designs are constrained by the uncertainty of whether the difference in sample means is relevant to all patients. This is a major complication in generalizing the resulting biomarkers to an out-of-sample individual preventing efficient individualized predictions of psychopathological deficits in clinical practice [15]. In response, current interest is shifting to individual-level variability/prediction of various brain diseases [16], [17], [18], [19], [20] and cognitive states [21], [22], [23] using neuroimaging-based machine learning methods. For instance, Cao et al., 2020 [13] assessed treatment response to antipsychotics of first-episode drug-naïve schizophrenia individuals by implementing a linear support vector classifier and functional connectivity features, reporting high prediction accuracy at the individual level. In addition, Meng et al., 2017 [24] using a multimodal feature fusion of MRI data introduced a regression analysis framework to estimate individualized clinical measures of patients with schizophrenia and achieved high prediction performance. More recently, an fMRI schizophrenia study incorporated multivariable regression in functional connectivity networks to predict the PANSS subscales, revealing predictive network-symptom associations [25]. From this standpoint, it is evident that individualized machine learning designs can not only promote the comprehension of the pathophysiological alterations characterizing schizophrenia, but also utilize idiosyncratic pattern variations to make predictions that could benefit the treatment and prognosis of affected individuals [26]. Taking all the above into consideration, this paper aspires to:

- explore the feasibility of inferring psychopathological deficits, as well as their progression using objective neuroimaging biomarkers at the individual level.
- investigate the progressive topological disruption of structural brain networks at the group level.

To that end, we developed a data-driven analysis framework incorporating an individualized-prediction model and graph-theoretical analysis approach based on structural brain networks derived from a longitudinal cohort with chronic schizophrenia. Unlike the majority of relative studies focusing on individual classification [27], this work proposes a generalized framework that explicitly predicts values of psychopathological deficits to meet the need for efficient and objective single subject prediction of brain disorders to eventually inform clinical decision-making. Specifically, we applied a strict Leave-One-Out Cross Validation (LOOCV) in a Connectome-based Prediction Models (CPMs) implementation to assess independent testing subjects' psychopathologic deficits prediction. Our results suggest that models based upon structural brain networks have the potential to be effective and generalizable predictors of psychopathological deficits, while also demonstrating SC features to be good prognostic biomarkers for establishing a reliable prediction model in longitudinal schizophrenia. Moreover, the topological analysis revealed a decreased network integration supporting the dysconnectivity hypothesis. To the best of our knowledge, this is the first study to comprehensively assess schizophrenia-related longitudinal changes of WM that putatively underlie the heterogeneous psychopathological deficits seen across individuals to produce group-consensus pathological maps.

II. Materials and Methods

A. Participants

The data collected in this work included participants from a longitudinal cohort study of schizophrenia [28], acquired in the Institute of Mental Health (IMH) – the sole state psychiatric hospital in Singapore. As such, seventy-six (76) patients with schizophrenia and 61 matched healthy participants were recruited at baseline. Among them, 38 patients and 39 controls participated in the follow-up study with a mean interval of about 5 years (individual scan intervals are presented in the Supplementary Materials, Fig. S1). No statistically significant difference of the interval was revealed between both groups. Patients were screened at baseline for alcohol or other substance abuse, as well as history of any significant neurological diseases. Healthy controls were recruited from the local community and the eligibility criteria also included no mental illness of any kind to first-degree relatives. The protocol of this study was approved by the Institutional Review Board of the IMH and was carried out according to the Declaration of Helsinki. Written informed consent was obtained from all participants.

B. Psychopathology Assessment

For all participants, presence or absence of psychopathology was established by a board-certified psychiatrist using information including the clinical history and medical records, examination of mental status, interviews with significant others, as well as the administration of the Structural Clinical Interview for DSM-IV disorders-Patients Version (SCID-P). The psychopathology and symptom severity was assessed using the Positive and Negative Syndrome Scale (PANSS)[3]. Briefly, PANSS is a widely-used 30-item clinician-rated instrument developed to provide comprehensive assessment of typological, dimensional and severity of schizophrenia. Here, the original three domains of PANSS was utilized to measure the symptomatology, namely positive, negative, and general psychopathology [29]. The positive syndrome consists of productive features superadded to the mental status (i.e., delusions, hallucinations, and disorganized thinking), the negative syndrome represents absence of normal functions (i.e., deficits in the cognitive, affective, and social levels), and the general syndrome contains items that assess the general

severity of psychopathology [3]. An overall score (i.e., overall = positive + negative + general) was also estimated to evaluate the symptom's overall severity. The PANSS scores of patients at both baseline and follow-up are presented in Supplementary Materials (Fig. S2).

C. MRI Acquisition

MRI scans were acquired on a 3-T Philips scanner (Achieva, Philip Medical System, The Netherlands) with an eight-element SENSE receiver head coil at the National Neuroscience Institute, Singapore. Prior scanning, subjects were instructed to keep still and remain as motionless as possible. Foam pads from the scanner manufacturer were applied to further minimize head motion. The following scanning settings were maintained for both baseline and follow-up data acquisition. Diffusion MRI images were recorded using a single-shot echo-planar sequence with the following parameters: repetition time (TR) / echo time (TE) = 3275 / 56 ms; flip angle = 90°; b-factor = 800 s/mm^2; 1 baseline image with b_0 = 0 s/mm^2) from 15 separate nonparallel directions; slice number = 42; thickness = 3 mm with no-gap; field of view (FOV) = 230 × 230 mm^2; acquisition matrix = 112 × 109, reconstructed to 256 × 256. For each participant, the diffusion sequences were scanned 3 times to improve the signal-to-noise ratio. A high-resolution T1-weighted magnetization prepared rapid gradient recalled echo sequence was used for structural MRI images acquisitions using the following parameters: TR / TE = 7200 / 3.3 ms; flip angle = 8°; slice number 180; thickness = 0.9 mm; FOV = 230 × 230 mm^2, in-plane resolution = 0.9 × 0.9 mm^2. The same scanner was used for the baseline (software version R2.6) and follow-up scans (software version R3.2).

D. Data Preprocessing

DTI data preprocessing was performed using the PANDA toolbox [30] and a previously-validated pipeline for diffusion MRI analysis [31], [32], [33]. In detail, the distortion of the diffusion weighted images were firstly corrected for head motion artifacts and eddy currents distortions using affine alignment to the b_0 image [34]. Then, a tensor was fitted to the diffusion profile within each voxel where the Fractional Anisotropy (FA) was estimated. Whole-brain tractography was subsequently performed using a deterministic streamline tracking algorithm (Fiber Assignment by Continuous Tracking, FACT) [35]. The tracking procedure started from the deep WM regions and terminated if it reached a voxel with a FA of < 0.15 or a turning angle higher than 45°[33]. To address the head motion artifacts on the brain images [36], we performed additional analysis, statistically comparing the head motion between both groups at baseline and followup. Notable no significant between-group differences were found at both time points ($p > 0.05$).

E. Structural Connectivity Estimation

For each participant, a structural brain network was generated by combining the individual parcellation map with the WM tractography (Fig. 1a). Specifically, a recently-introduced connectivity-based parcellation scheme suitable for connectivity and/or brain network analyses [37], [38], [39] was employed to parcellate the entire gray matter into 246 regions-of-interest (ROIs, 123 in each hemisphere) and define the network nodes. The individual-based parcellation template was obtained through weaving the brainnetome atlas from the standard MNI space to subject DTI native space. From the reconstructed fiber tracts, Structural Connectivity (SC) was defined as the streamline density to account for the different sizes of the ROIs [40]. For any pair of ROIs (i.e., node i and j), the SC weight w_{ij} was estimated as the ratio between the number of streamlines ($\geq$ 3 fiber tracks) and the sum of volumes of node i and j. As such, each individual SC network reflected a symmetric 246 $\times$ 246 matrix.

F. Individualized Prediction of Psychopathological Deficits

The previously-validated Connectome-based Prediction Model (CPM) was implemented for the prediction of psychopathological deficits [26]. To address the prognosis on an individual level (i.e., verify if psychopathological deficits of a previously unseen patient could be reliably predicted from the SC profile), a strict LOOCV approach was utilized. In this manner, data from one subject were excluded to generate the CPM, while testing was performed in the out-of-sample patient data. The LOOCV framework employed was performed separately on all the four PANSS scores (i.e., positive, negative, general, and overall), with each CPM iteration including a masking (feature selection), a subject-based feature summarization, a model fitting and a prediction step (Fig.1b, 1c). In detail, data (SC matrices and PANSS scores) from one patient were appointed as the out-of-sample (test set) and feature selection was performed on the remain-ing n-1 patients (training set). Prior to the feature selection and mask estimation, testing for normality was applied on both SC matrices and PANSS scores, revealing a non-normal PANSS scores distribution. As such, the feature selection procedure utilized a non-parametric Kendall Tau correlation, thereby associating each edge in the connectivity matrices to the psychopathological scores and identifying the most important edges via a threshold, thus generating a significance association mask. This mask was subsequently applied to the individual connectivity matrix of each patient, with the obtained prominent edges being summarized into a single value for each subject in the training set. A predictive model was then built by linear fitting the single-subject summary values of SC features and the corresponding psychopathology scores assuming a linear relationship between them. To further validate the reliability of the model, additional analyses were performed at a various statistical thresholds ($p < 0.05$, $p < 0.01$, $p < 0.005$) ensuring that the results obtained were not specific to the chosen threshold. According to [26], a threshold of $p < 0.01$ that is not too conservative (excluding useful SC features) nor too loose (including spurious SC features) were adopted here. Validation analyses using $p < 0.05$ and $p < 0.005$ are presented in Supplementary Materials (Table S4). Additionally, potential confounding factors (including head motion, age, gender, and handedness) were regressed out

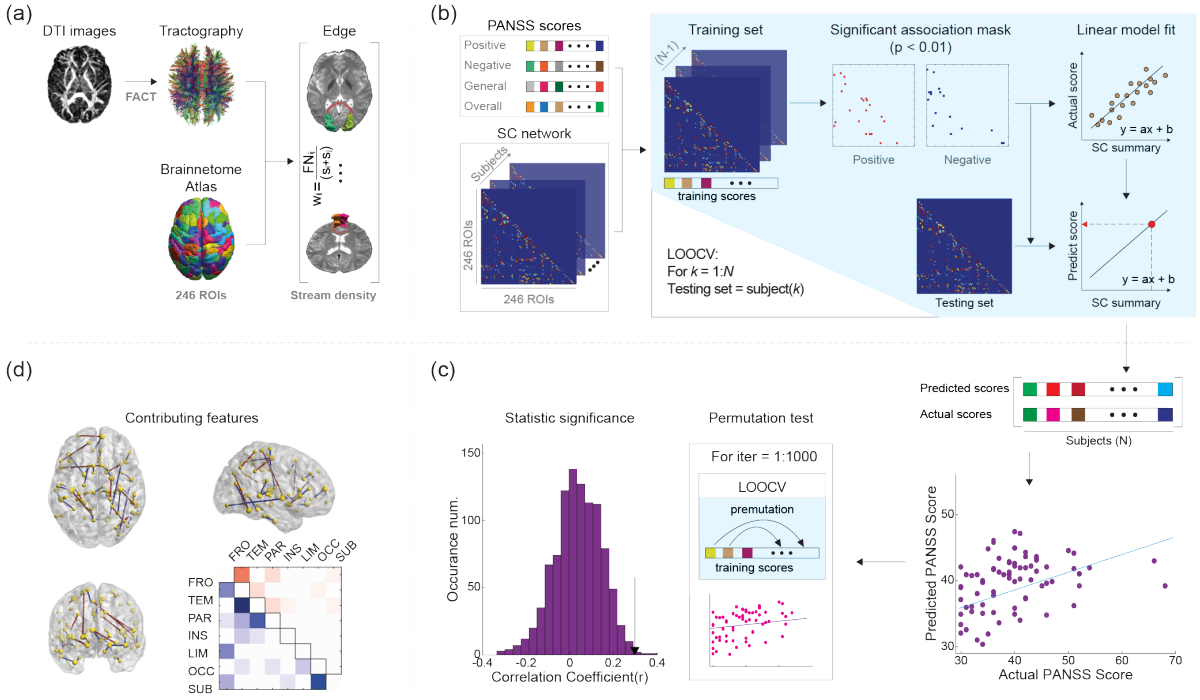

Fig. 1. A schematic of the framework adopted. In (a) the SC network was constructed by estimating the fractional anisotropy and assigning the fibers by obtaining the whole-brain tractography, while node definition was implemented using the Brainnetome atlas at the individual-level. Edge between any pair of nodes was defined as the streamline density. In (b) the LOOCV CPM approach was implemented for all the four PANSS scores. Each edge was correlated to the psychopathological scores and a significant association mask was then created and applied to each patient, while summarizing the important features into a single value. A predictive linear model was then built and applied on the Testing set to estimate the predicted psychopathological score. In (c) The prediction performance was assessed as well as the statistical significance (via permutation tests). In (d) The most significant SC features in terms of their contribution to the schizophrenia modeling were also determined.

prior to the model construction. It is noteworthy mentioning that the significant associations could be both positive and negative, hence, separate prediction models for each dimension of symptom were estimated employing only positive, negative, general and overall features. The obtained predictive model was then applied on the SC summary value of the out-of-sample testing set to estimate the predicted PANSS score. The abovementioned procedure was replicated n-times until each patient was selected as testing set. A schematic overview of the LOOCV CPM prediction framework is presented in Fig.1

After completing all iterations, prediction performance was assessed via the Pearson correlation coefficient (r) and the mean absolute error (MAE) of the actual and predicted PANSS scores [21], [37]. Specifically, the aforementioned prediction procedure was applied 1,000 times, permuting the psychopathologic scores corresponding to the SC across the training samples without replacement. Statistical significance was determined as the ratio of the obtained results being better than those expected by chance [41]. In this regard, the p-value for r (p_r) was determined as the number of iterations that showed a higher value of correlation coefficients than the actual r. By contrast, the p-value (p_{MAE}) for the MAE was determined as the number of iterations that showed a lower MAE than the actual value. Given the fact that separate prediction models were constructed among different psychopathologic scores at baseline and follow-up, the permutation test was conducted separately.

The primary focus of the current work is to assess the utility of SC as a biomarker to predict psychopathological deficits (as indicated by the PANSS scores) of patients with schizophrenia and additionally investigate the longitudinal effects of schizophrenia on the corresponding SC features. To that end, two separate prediction paradigms were employed in the current work. At baseline, the psychopathological scores were set as input for generating the CPM model to fulfill the first objective. Next, the changes of psychopathological scores (ΔPANSS = PANSS$_{Follow-up}$ – PANSS$_{Base}$) were chosen as input for the CPM model estimation at follow-up, in order to study the longitudinal effects of schizophrenia on the corresponding SC features and thus predict the changes of psychopathological deficits.

To better interpret the complex neural mechanisms of schizophrenia, we identified the most prominent SC features with respect to their contribution to the prediction modeling. Heuristically, separate prediction models for each dimension of symptoms would lead to dissimilar set of contributing features (Fig. 1d). As such, the designation of the important features was performed separately for each prediction model (i.e., positive, negative, general and overall). Since the set of contributing SC features would be slightly different in each LOOCV iteration, a threshold for group consistency (i.e., the ratio between the appearance of the feature and the total number of the iteration) was defined to obtain the most salient features, determined at 90%.

TABLE I
PREDICTION PERFORMANCE AT BASELINE.

	$PANSS_{positive}$		$PANSS_{negative}$		$PANSS_{overall}$	
	Negative Features	Both Features	Positive Features	Both Features	Negative Features	Both Features
r (p_r)	0.327 (0.002)	0.349 (<0.001)	0.392 (<0.001)	0.353 (0.001)	0.343 (0.002)	0.280 (0.014)
MAE (p_{MAE})	2.687 (0.004)	2.705 (<0.001)	1.992 (0.002)	2.174 (0.026)	5.535 (<0.001)	5.858 (0.007)

Note: Statistical significance was estimated using 1,000 permutation tests for the obtained prediction performance (r, MAE)

G. Graph Theoretical Analysis

In order to assess the effects of schizophrenia on SC at a group level, we investigated the alterations in SC in terms of network topology through a graph theoretical analysis approach on the obtained structural brain network. In this regard, a unified efficiency method was employed on both global and local levels to estimate the information transfer efficiency [42]. Specifically, the global efficiency (E_{glob}) was adopted as a measure of parallel information effectiveness transfer in the network, while the local efficiency (E_{loc}), as a measure of information exchange at the clustering level [43] (the detailed interpretations and mathematical definitions of global and local efficiency are provided in the Supplementary Materials). To quantitatively evaluate network measures significant effects, a general linear model (GLM) comprising of factor #1 group (patients vs. controls), factor #2 session (baseline vs. follow-up) and their interaction (group-by-session) was applied on all the data, with gender, handedness and baseline age set as covariates. In order to reduce the inter-subject variance, we performed an additional within-subject design GLM with the same factors of group and session on the subjects participating in both scans (baseline and follow-up). If any significant main effect was found (p_{GLM} ¡ 0.05), further post-hoc tests were performed. A value of $p_{GLM} < 0.05$ was considered significant. In addition, a false discovery rate (FDR) threshold of q = 0.05 was utilized for the correction of multiple comparisons. All statistical analyses of network measures were performed using SPSS 23 software.

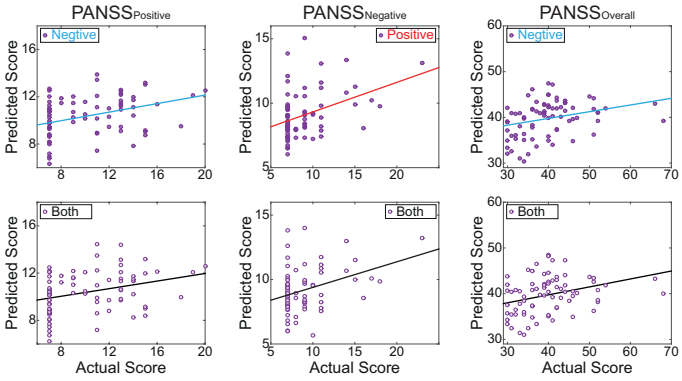

Fig. 2. Prediction performance of the CMP models for the significantly correlated predicted and actual PANSS scores at baseline.

III. RESULTS

A. Prediction Performance

Based on the CPM framework implemented, we found that the predicted positive ($PANSS_{positive}$), negative ($PANSS_{negative}$), and overall ($PANSS_{overall}$) scores were highly correlated with the actual scores at baseline, yet with distinct SC feature patterns (Table I, Fig. 2). Prediction model for $PANSS_{general}$, however, failed to obtain significant findings. Specifically, the predicted $PANSS_{positive}$ and $PANSS_{overall}$ scores were highly correlated with the actual scores when using negative SC features (r = 0.327, p_r = 0.002 and 0.343, $p_r < 0.001$ respectively) or both positive and negative SC features (r = 0.349, p_r = 0.002 and 0.280, p_r = 0. 014 respectively). The corresponding MAEs for $PANSS_{positive}$ were 2.687 and 2.705, which were significantly lower than those expected by chance ($p_{MAE} <$ 0.005), whereas $PANSS_{overall}$ MAEs were 5.535 and 5.858 with similar significance level ($p_{MAE} < 0.01$). On the other hand, significant associations between the predicted and actual $PANSS_{negative}$ scores were revealed when using positive (r = 0.392, $p_r < 0.001$) or both positive and negative SC features (r = 0.353, p_r = 0.001). Similar to positive and overall predicted scores, error estimations for $PANSS_{negative}$ were also significantly lower than those expected by chance ($p_{MAE} < 0.05$) with MAEs being 1.992 and 2.174.

At follow-up, the predicted $\Delta PANSS_{positive}$ and $\Delta PANSS_{overall}$ were found to be highly correlated with the actual changes when using both positive and negative SC features (r = 0.412, $p_r < 0.001$ and 0.329, p_r = 0.010 respectively) (Table II). The additional analyses of the prediction models also demonstrated statistically significant MAEs for $\Delta PANSS_{positive}$ (2.892, $p_{MAE} < 0.01$) and $\Delta PANSS_{overall}$ (7.593, p_{MAE} = 0.038). In contrast, the prediction model for $\Delta PANSS_{negative}$ failed to pass the significance threshold. Additional information regarding the statistical tests of the prediction performance at baseline and follow-up are presented in Supplementary Materials (Fig. S3 and Fig. S4).

TABLE II
PREDICTION PERFORMANCE AT FOLLOW-UP.

	$\Delta PANSS_{positive}$	$\Delta PANSS_{overall}$
	Both Features	Both Features
r (p_r)	0.412 (<0.001)	0.329 (0.010)
MAE (p_{MAE})	2.892 (<0.001)	7.593 (0.038)

B. Structural Connectivity Features

At baseline (Fig. 3), 45 SC features were found to be the most important for predicting the $PANSS_{positive}$, among which 34 features exhibited significantly negative association with $PANSS_{positive}$ scores (i.e., the more severe the symptoms

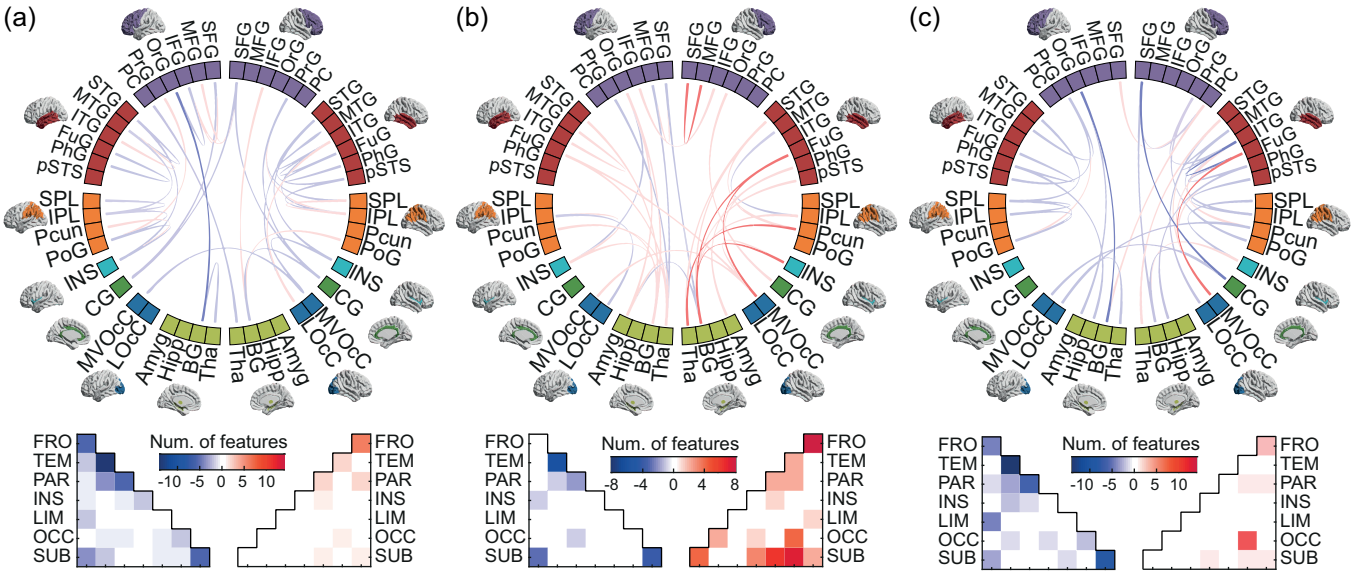

Fig. 3. Circle plot visualization of the most prominent SC features and their distributions in the baseline prediction model for (a) PANSS$_{positive}$, (b) PANSS$_{negative}$, and (c) PANSS$_{overall}$. Positive (red) and negative (blue) features are drawn between the nodes. The nodes are color coded according to their cortical lobes. The full names of the abbreviated regions of interest could be found in Table S3.

the lower the feature weight). The remaining positive associations features (11 out of 45), presented a frontal lobe connectivity majority. Overall topographic analysis demonstrated a broad distribution within temporal, parietal, and subcortical areas as well as between frontal and limbic brain regions. For the PANSS$_{overall}$ prediction model, 50 SC features were designated as the most prominent. In detail, the identified SC features were mainly negative associated features (39 out of 50) with a widespread involvement of brain regions that resided within temporal, parietal and subcortical areas, as well as between frontal and parietal/subcortical regions. Positive SC features, on the other hand, showed a right-hemispheric predominance, connecting temporal and occipital regions. Interestingly, among the 48 most contributive SC features for PANSS$_{negative}$ prediction model, the majority of them (36 out of 48) exhibited significantly positive association with the symptom scores, with the topological distribution involving brain regions within and between the frontal, temporal, and subcortical areas.

Similar to baseline, the prediction for PANSS$_{positive}$ alterations at follow-up (Fig. 4) displayed a majority of negative SC features, with 23 out of the total of 36 SC features exhibiting significant negative associations. Relative to the designated brain areas, the negative features presented a right-hemispheric majority, mainly located in the temporal and subcortical regions as well as between occipital and subcortical regions. In contrast, the positive SC features for ΔPANSS$_{positive}$ prediction model demonstrated a left-hemispheric tendency and mainly resided in frontal and temporal lobes. For the ΔPANSS$_{overall}$ prediction model at follow-up, we found 33 evenly distributed SC features contributing to the model, with 15 of them being negative and 18 positive features. Spatial distribution analysis of the features indicated the negative features to be mainly located in the limbic region, as well as between subcortical and occipital lobes. On the contrary, left-hemisphere was mostly involved regarding positive SC features, primarily including frontal, temporal parietal and subcortical regions, in addition to between temporal and insular lobes, between frontal and occipital lobes, and between frontal and subcortical areas. The spatial distribution of the most prominent SC features for baseline and follow-up psychopathological deficits prediction are presented in Supplementary Materials Fig. S5 and Fig. S6.

C. Network Reorganization

The additional analyses of the network metrics presented significant main group (SCZ $<$ NC) effect in both E_{glob} ($F_{1,207}$ = 83.106, $p_{GLM} < 0.001^{*}$; * indicates survive FDR threshold at q < 0.05) and E_{loc} ($F_{1,207}$ = 12.205, $p_{GLM} = 0.001^{*}$), whereas a significant effect of session was only revealed in E_{loc} ($F_{1,207}$ = 4.610, p_{GLM} = 0.033), suggesting an intrinsic deficit of network efficiency in patients with schizophrenia (Table III). Interestingly, significant group-by-session interaction effect was revealed in E_{glob} ($F_{1,207} = 6.345$, $p_{GLM} = 0.013^{*}$). Post-hoc analysis shows that this sig-nificant interaction resulted from different development trends in patient and control groups, i.e., patients with schizophrenia exhibited a significant longitudinal reduction of E_{glob} (t_{112} = 2.727, p = 0.007) in comparison to a preserved E_{glob} in controls (t_{98} = -0.447, p = 0.656).

In order to reduce the inter-subject variance, we further applied an additional within-subject design GLM. Similar to our main findings, significant main group (SCZ $<$ NC) effect was observed in E_{glob} ($F_{1,147}$ = 88.147, $p_{GLM} < 0.001^{*}$) and E_{loc} ($F_{1,147}$ = 17.427, $p_{GLM} < 0.001^{*}$), whereas significant main session (Baseline $>$ Follow-up) effect was revealed in

TABLE III
COMPARISON OF LONGITUDINAL BRAIN NETWORK TOPOLOGICAL CHANGES BETWEEN BOTH GROUPS.

Metrics	GLM model on all data			Within-subject GLM		
	Group effect F1,207 (p_{GLM})	Session effect F1,207 (p_{GLM})	Interaction F1,207 (p_{GLM})	Group effect F1,147 (p_{GLM})	Session effect F1,147 (p_{GLM})	Interaction F1,147 (p_{GLM})
E_{glob}	**83.106 (<0.001)** ↑	2.299 (0.131)	**6.345 (0.013)**	**88.147 (<0.001)** ↑	2.831 (0.095)	**4.176 (0.043)**
E_{loc}	**12.205 (0.001)** ↑	**4.610(0.033)** ◁	0.109 (0.742)	**17.427 (<0.001)** ↑	**5.340 (0.022)** ◁	0.176 (0.675)

Note:Significant effects ($p_{GLM} < 0.05$) were indicated in **bold**. ↑ indicates NC > SCZ; ◁ indicates follow-up < baseline.

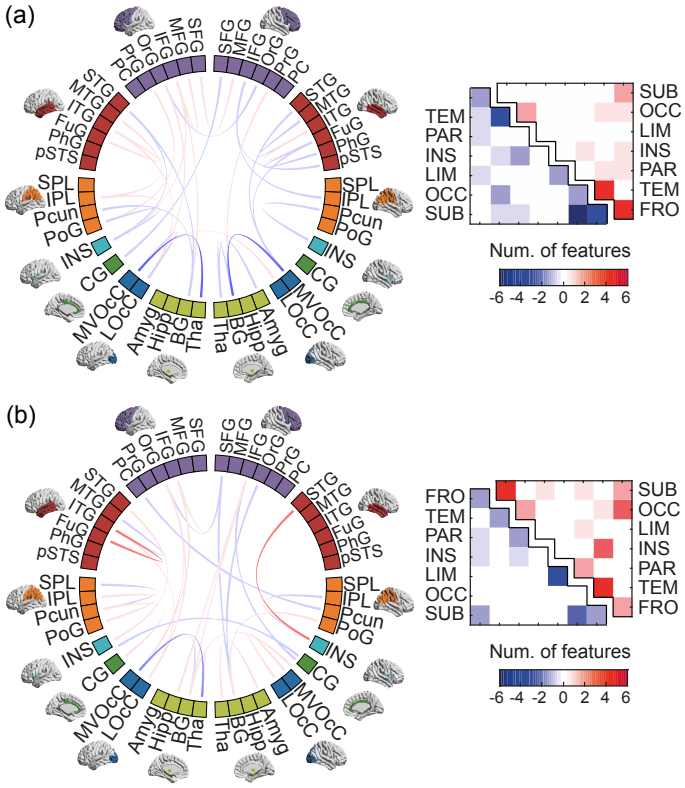

Fig. 4. Circle plot visualization of the most prominent SC features in the follow-up prediction model for (a) $\Delta\text{PANSS}_{positive}$ and (b) $\Delta\text{PANSS}_{overall}$. Positive (red) and negative (blue) features are drawn between the nodes. The nodes are color coded according to their cortical lobes.

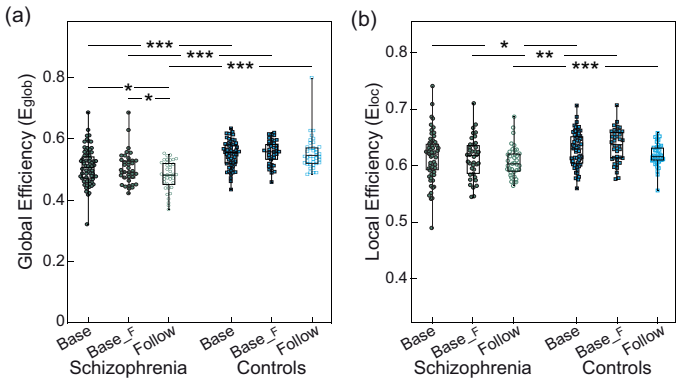

Fig. 5. Box plots of (a) Global efficiency (E_{glob}) and (b) Local efficiency (E_{loc}), with the whiskers presenting interquartile range and the line within each box marking the median value of the distribution. Base: all subjects at baseline; Base_F: subjects at baseline who finished follow-up scan; Follow: subjects at follow-up. $*$ p < 0.05; $**$ p < 0.01; $***$ p < 0.001.

E_{loc} ($F_{1,147} = 5.340$, $p_{GLM} = 0.022^{*}$). Again, a significant group-by-session interaction was revealed in E_{glob} ($F_{1,147} = 4.176$, $p_{GLM} = 0.043$) (Fig. 5).

IV. DISCUSSION

Using a longitudinal cohort of chronic schizophrenic patients, we successfully built a SC-based regression model that efficiently captures the individual differences in psychopathologic deficits as well as their progression. Moreover, the SC analysis allowed for a direct examination of the architecture of the constructed network, quantitatively assessing the associated topological properties and effects of schizophrenia. To the best of our knowledge, this is the first time that individualized prediction modeling of psychopathologic deficits has been applied to investigate the progressive schizophrenia anatomical connectome alterations. The obtained results provide new evidence to support the dysconnectivity hypothesis and highlight the potential of structural brain networks as a holistic neural index in unraveling the pathophysiologic mechanisms of schizophrenia.

A. Psychopathologic Deficits Modeling

Aberrations of WM characteristics are increasingly implicated in schizophrenia, and may be the neuropsychiatric basis for symptom severity [44], [45]. With regard to the CPM prediction performance, the correlation coefficient between the actual and the prediction scores both in baseline and follow-up (mean correlation value ≈ 0.35) are analogous to the majority of relative regression studies [25], [46], [47]. This fact, in conjunction with the very low p-values derived from the permutation tests, suggest that the adopted models were able to detect affiliations between the PANSS scores and the selected SC edges effectively. In line with previous studies, we found that positive, negative and overall symptoms were related to SC features with distinct patterns. Positive symptoms in schizophrenia are characterized by misperception of internal stimuli [3], whereas negative symptoms often represent loss of normal function [48], both of which have long been recognized to be associated with deficits in multiple types of WM tracts [49] and functional connectivity [50]. In this regard, the observations of different SC features among the prediction models, particularly the contrast of dominant SC feature patterns between positive and negative symptoms may indicate distinct pathophysiological mechanisms in schizophrenia [4]. We speculate that the dominant negative SC features in predicting positive symptoms (i.e., the higher positive symptoms, the lower SC weights) suggest a relaxation of normal constraints imposed by anatomical interactions on brain function,

while dominant positive SC features in negative symptoms prediction model (i.e., the higher negative symptoms, the higher SC weight) may be indicatory of restricted anatomical interactions that disrupt dynamic brain function [51], [32]. Interestingly, we found an increased proportion of positive SC features in the prediction model for the longitudinal changes of psychopathological deficits. Given the fact that both positive and overall symptoms showed significant improvements in the follow-up (Fig. S2 in Supplementary Materials), the observed trend further implicates the positive SC features suggesting that the more reduced symptom severity the higher SC features at follow-up. Moreover, considering that the majority of the reduced SC features were predictive for both positive and overall symptom severity at baseline, the preserved SC features could indicate an association with improved psychopathological deficits.

Regarding the regional anatomical analysis of the prominent SC features, the widespread distribution across various systems is hardly surprising due to the fact that schizophrenia is a complex neuropsychiatric disorder with extensive clinical manifestations in multiple domains [1]. For instance, Meng et al., 2017 [24] recently reported a prediction model based upon multimodal neuroimaging data and found brain areas likely responsible for PANSS symptoms of schizophrenia that included cingulate, subcortical, frontal and parietal areas that largely overlap with our findings. It is noteworthy that the majority of prior studies that report widespread aberrations of WM have utilized a classification/comparison scheme that appears to emphasize group differences between patients and controls [52]. The individualized prediction scheme used in the current work amplifies individual differences in symptomatology showing consistent findings with previous studies[24], [4].

B. Network Topology

Conceptually, network efficiency is a measure of information transmission [42]. The significantly reduced network efficiency in patients (at both global and local levels) denotes a disrupted communication between segregated parts of the brain. This is consistent with previous observations from cross-sectional structural network studies [5], [44], [7]. In fact, a meta-analysis of DTI studies in schizophrenia [53] investigated a total of 407 patients and reported 2 significantly reduced WM clusters: the cerebello-thalamo-cortical circuit and a temporal network interconnecting the frontal lobe, insular, hippocampus-amygdala, and temporal and occipital lobes, indicating macrocircuit WM deficits in schizophrenia. Consequently, the brain networks of patients developed toward a less integrated architecture with preserved local efficient architecture at follow-up. More recently, a study investigating the regional distribution of WM abnormalities in 1,963 schizophrenia patients from 29 independent international research works identified widespread (i.e., 20 out of 25 major WM fasciculi) significant reductions in WM [44]. Notably, the network local efficiency does not show significant difference in the follow-up. This fact, taken together with the longitudinal prediction models findings, infers that the preserved SC features might lead to unvarying efficiency in the local level over time. By contrast, the accelerated dysconnectivity at the global level is also consistent with our prior observations from a small longitudinal cohort [31]. Although the extent of relevant works is extremely limited, hindering the acquisition of conclusive evidence, our results were in line with studies of longitudinal volumetric [54], [55] and WM [56] deficits in schizophrenia. In this regard, Olabi et al., 2011 [55] showed progressive brain volume reduction in a meta-analysis investigating 27 studies with a total of 928 patients, with other relevant works reported similar longitudinal decrements in volume in multiple neocortical regions [11], [54]. Furthermore, using a cross-sectional chronic schizophrenia cohort with comparable age range, Cropley et al., 2017 [57] investigated the influence of age on brain alterations and reported gray and WM significant deterioration at a faster rate with age. On this premise the progressive degradation of brain structure with age in schizophrenia has been widely recognized [58]. Contemporary theories suggest that the complex clinical presentations of schizophrenia are related to aberrant connectivity between distinct brain regions – the dysconnectivity hypothesis [6], which emphasize the degradation of the brain's integrative processes in the pathophysiology of schizophrenia. In this context, our findings of a longitudinal trend toward decreased global integration adds to earlier works and provides new evidence supporting the notion of schizophrenia as a disconnection syndrome [59].

C. Implications and Future Considerations

Some issues should be considered when interpreting our findings. First and foremost, to obtain a stable individualized prediction model, a large longitudinal cohort was used that might potentially introduce some confounding factors such as different medication dosages amongst patients. Of note is that previous neuroimaging studies have reported deviations in localized brain regions and connections due to pharmacological treatment, with mixed findings regarding whether antipsychotics have neuroprotective or neurodegenerative effects [60], [61]. It is therefore not possible to draw conclusions pertaining to the influence of medication on brain anatomical aberrations [10]. In fact, Rubinov et al., 2009 [62] suggested that medication is unlikely to be a confounding factor and may instead exert a normalizing influence on the brain connectome. On this premise, we performed additional analysis to estimate the associations between the medication dosage and psychopathological deficits and found no significant relationships (Table S2 in Supplementary Materials). The obtained observations suggest a reflection of the intrinsic disease process instead of an effect of direct pharmacological treatment. Nevertheless, caution is needed when considering the potential confounding factor of longer periods of treatment and different doses of antipsychotics or epiphenomena related to the illness.

Furthermore, in this study the SC was reconstructed using a computationally inexpensive deterministic tractography method that is known to have limited capacity in handling complex fiber architectures [35]. This may in turn result in an under-representation of the SC weights with reduced connectome sensitivity [63]. We assessed the credibility of our

tracking results through checking the well-known WM fiber bundles (data not shown) and found that the reconstructed fiber bundles correspond accurately to the human WM anatomy from previous studies [64], [65]. In contrast, probabilistic tractography might be superior in addressing the fiber crossing issues, but yields dense connectomes with reduced connectome specificity. In fact, a relevant study showed that connectome specificity is at least twice as important as connectome sensitivity with respect to the analysis of brain connectomes [66]. Further work with cautious application of advanced probabilistic fiber tracking methods and crossing-fiber models to high-quality data could therefore provide more insight in the complex brain architectures of schizophrenia. Moreover, a previously-validated stream density (i.e., normalized FN by the size of the interconnected ROIs) approach [40] was adopted here for estimating the SC weight. Additional analyses of the individualized prediction model performance against different methods for SC weight estimation (utilizing FA for the SC weight) obtained similar results (Table S5 in Supplementary Materials). Heuristically, FN is an index to reflect the WM structure [67], while FA reflects the fibre integrity [68] and is highly correlated with conductivity [69]. In this regard, the validation analyses indicates that the individualized SC prediction model could capture the intrinsic aberrations of WM, serving as potential biomarkers for symptom assessment in patients with schizophrenia.

Finally, since this study is the first exploratory investigation of individualized prediction of psychopathological deficits in a longitudinal cohort of schizophrenia in stable phase, its primary objective was to demonstrate the feasibility of utilizing SC to predict individual clinical symptoms. On this premise, a previously-validated CPM method [26] was adopted on a self recorded longitudinal dataset [28]. Compared to other regression methods, CPM proved superior in terms of the low computational cost and the effectiveness of readily interpretable information pertaining to the importance of the features. However, the current models can not sufficiently replace relevant clinical tests, despite most of our predictions reaching an acceptable statistical effect size (i.e., $r > 0.3$) [70]. Future works are therefore encouraged to keep improving the accuracy and generalizability of the current work via the integration of multimodal neuroimaging data [24] and clinical variables [71], thus promoting an operational model for objective assessment of symptom severity in schizophrenia. More importantly, previous studies showed that adequate statistical power of prediction accuracy and its stability were increased with sample size [37], [18]. For instance, in [24] a generalized framework of multiple modalities neuroimaging data was reported to efficiently predict cognitive and symptom scores in a modestly sized schizophrenia sample. Moreover, an uncorrected p-value of 0.05 was employed for establishing the significance and presenting the graph theoretical analysis results. In this regard, interpreting these findings should be done with caution. Taking this into consideration, we mainly focused on the interpretation of the resulting patterns and highlighted those that survived corrections for multiple comparisons. In this respect, future studies that incorporate large independent study samples, different prediction methods and diverse neuroimaging data could further validate our findings and ensure the generalizability of the prediction model in practice.

V. Conclusion

In this paper, an individualized SC model for the prediction of psychopathological deficits in a longitudinal cohort was employed, allowing the identification of potential biomarkers for symptom assessment and prognostic evaluation of illness progression. As such, the framework proposed was able to lead to comprehensive appreciations that give insights into the pathophysiologic mechanisms of schizophrenia and how it evolves in time. More importantly, it provided group-level evidence of progressive disruption of brain anatomical networks in patients with schizophrenia by quantitatively estimating SC aberrations, supporting the dysconnectivity hypothesis. Taken together, the individualized prediction models offer the opportunity for the quantitative translation of neuroimaging data into diagnostic and prognostic tools, providing a more complete appreciation of the brain neural mechanisms and how they manifest and evolve throughout lifetime.

References

[1] O. D. Howes and R. M. Murray, "Schizophrenia: an integrated sociodevelopmental-cognitive model," *Lancet*, vol. 383, no. 9929, pp. 1677–1687, May 2014.

[2] T. R. Insel, "Rethinking schizophrenia," *Nature*, vol. 468, no. 7321, pp. 187–193, 2010.

[3] S. R. Kay, A. Fiszbein, and L. A. Opler, "The positive and negative syndrome scale (PANSS) for schizophrenia," *Schizophr Bull*, vol. 13, no. 2, pp. 261–276, 1987.

[4] D. Wang, M. Li, M. Wang, F. Schoeppe, J. Ren, H. Chen, D. Öngür, R. O. Brady, J. T. Baker, and H. Liu, "Individual-specific functional connectivity markers track dimensional and categorical features of psychotic illness," *Mol Psychiatry*, vol. 25, no. 9, pp. 2119–2129, Sep. 2020.

[5] A. Fornito, A. Zalesky, C. Pantelis, and E. T. Bullmore, "Schizophrenia, neuroimaging and connectomics," *Neuroimage*, vol. 62, no. 4, pp. 2296–2314, Oct. 2012.

[6] K. Friston, H. R. Brown, J. Siemerkus, and K. E. Stephan, "The dysconnection hypothesis (2016)," *Schizophr Res*, vol. 176, no. 2-3, pp. 83–94, Oct. 2016.

[7] M. P. van den Heuvel and A. Fornito, "Brain networks in schizophrenia," *Neuropsychol Rev*, vol. 24, no. 1, pp. 32–48, Mar. 2014.

[8] E. Bullmore and O. Sporns, "Complex brain networks: graph theoretical analysis of structural and functional systems," *Nat Rev Neurosci*, vol. 10, no. 3, pp. 186–198, Mar. 2009.

[9] R. J. Duchatel, C. Shannon Weickert, and P. A. Tooney, "White matter neuron biology and neuropathology in schizophrenia," *npj Schizophr*, vol. 5, no. 1, pp. 1–9, Jul. 2019.

[10] B. Dietsche, T. Kircher, and I. Falkenberg, "Structural brain changes in schizophrenia at different stages of the illness: A selective review of longitudinal magnetic resonance imaging studies," *Aust N Z J Psychiatry*, vol. 51, no. 5, pp. 500–508, May 2017.

[11] N. C. Andreasen, P. Nopoulos, V. Magnotta, R. Pierson, S. Ziebell, and B.-C. Ho, "Progressive brain change in schizophrenia: a prospective longitudinal study of first-episode schizophrenia," *Biol Psychiatry*, vol. 70, no. 7, pp. 672–679, Oct. 2011.

[12] G. Cattarinussi, G. Delvecchio, C. Prunas, and P. Brambilla, "Effects of pharmacological treatments on neuroimaging findings in first episode affective psychosis: A review of longitudinal studies," *J Affect Disorders*, 2020.

[13] B. Cao, R. Y. Cho, D. Chen, M. Xiu, L. Wang, J. C. Soares, and X. Y. Zhang, "Treatment response prediction and individualized identification of first-episode drug-naïve schizophrenia using brain functional connectivity," *Mol Psychiatry*, vol. 25, no. 4, pp. 906–913, Apr. 2020.

[14] T. Wolfers, J. K. Buitelaar, C. F. Beckmann, B. Franke, and A. F. Marquand, "From estimating activation locality to predicting disorder: A review of pattern recognition for neuroimaging-based psychiatric diagnostics," *Neurosci Biobehav Rev*, vol. 57, pp. 328–349, Oct. 2015.

[15] J. Lv, M. Di Biase, R. F. H. Cash, L. Cocchi, V. L. Cropley, P. Klauser, Y. Tian, J. Bayer, L. Schmaal, S. Cetin-Karayumak, Y. Rathi, O. Pasternak, C. Bousman, C. Pantelis, F. Calamante, and A. Zalesky, "Individual deviations from normative models of brain structure in a large cross-sectional schizophrenia cohort," *Mol Psychiatry*, Sep. 2020.

[16] M. R. Arbabshirani, S. Plis, J. Sui, and V. D. Calhoun, "Single subject prediction of brain disorders in neuroimaging: Promises and pitfalls," *Neuroimage*, vol. 145, no. Pt B, pp. 137–165, Jan. 2017.

[17] R. Chen, Z. Cui, L. Capitão, G. Wang, T. D. Satterthwaite, and C. Harmer, "Precision biomarkers for mood disorders based on brain imaging," *BMJ*, vol. 371, p. m3618, Oct. 2020.

[18] J. Dubois and R. Adolphs, "Building a Science of Individual Differences from fMRI," *Trends Cogn Sci*, vol. 20, no. 6, pp. 425–443, Jun. 2016.

[19] J. Sui, R. Jiang, J. Bustillo, and V. Calhoun, "Neuroimaging-based Individualized Prediction of Cognition and Behavior for Mental Disorders and Health: Methods and Promises," *Biol Psychiatry*, vol. 88, no. 11, pp. 818–828, Dec. 2020.

[20] M. Antonakakis, S. Schrader, Ü. Aydin, A. Khan, J. Gross, M. Zervakis, S. Rampp, and C. H. Wolters, "Inter-subject variability of skull conductivity and thickness in calibrated realistic head models," *Neuroimage*, vol. 223, p. 117353, 2020.

[21] Z. Cui, M. Su, L. Li, H. Shu, and G. Gong, "Individualized Prediction of Reading Comprehension Ability Using Gray Matter Volume," *Cereb Cortex*, vol. 28, no. 5, pp. 1656–1672, May 2018.

[22] E. S. Finn, X. Shen, D. Scheinost, M. D. Rosenberg, J. Huang, M. M. Chun, X. Papademetris, and R. T. Constable, "Functional connectome fingerprinting: identifying individuals using patterns of brain connectivity," *Nat Neurosci*, vol. 18, no. 11, pp. 1664–1671, Nov. 2015.

[23] I. Tavor, O. Parker Jones, R. B. Mars, S. M. Smith, T. E. Behrens, and S. Jbabdi, "Task-free MRI predicts individual differences in brain activity during task performance," *Science*, vol. 352, no. 6282, pp. 216–220, Apr. 2016.

[24] X. Meng, R. Jiang, D. Lin, J. Bustillo, T. Jones, J. Chen, Q. Yu, Y. Du, Y. Zhang, T. Jiang, J. Sui, and V. D. Calhoun, "Predicting individualized clinical measures by a generalized prediction framework and multimodal fusion of MRI data," *Neuroimage*, vol. 145, no. Pt B, pp. 218–229, Jan. 2017.

[25] J. Chen, V. I. Müller, J. Dukart, F. Hoffstaedter, J. T. Baker, A. J. Holmes, D. Vatansever, T. Nickl-Jockschat, X. Liu, B. Derntl, L. Kogler, R. Jardri, O. Gruber, A. Aleman, I. E. Sommer, S. B. Eickhoff, and K. R. Patil, "Intrinsic connectivity patterns of task-defined brain networks allow individual prediction of cognitive symptom dimension of schizophrenia and are linked to molecular architecture," *Biol Psychiatry*, vol. 89, no. 3, pp. 308–319, Feb. 2021.

[26] X. Shen, E. S. Finn, D. Scheinost, M. D. Rosenberg, M. M. Chun, X. Papademetris, and R. T. Constable, "Using connectome-based predictive modeling to predict individual behavior from brain connectivity," *Nat Protoc*, vol. 12, no. 3, pp. 506–518, Mar. 2017.

[27] A. Riecher-Rössler and E. Studerus, "Prediction of conversion to psychosis in individuals with an at-risk mental state: a brief update on recent developments," *Curr Opin Psychiatry*, vol. 30, no. 3, pp. 209–219, May 2017.

[28] N. F. Ho, J. E. Iglesias, M. Y. Sum, C. N. Kuswanto, Y. Y. Sitoh, J. De Souza, Z. Hong, B. Fischl, J. L. Roffman, J. Zhou *et al.*, "Progression from selective to general involvement of hippocampal subfields in schizophrenia," *Mol Psychiatry*, vol. 22, no. 1, pp. 142–152, 2017.

[29] S. R. Kay, L. A. Opler, and J.-P. Lindenmayer, "The positive and negative syndrome scale (PANSS): rationale and standardisation," *Brit J Psychiatry*, vol. 155, no. S7, pp. 59–65, 1989.

[30] Z. Cui, S. Zhong, P. Xu, G. Gong, and Y. He, "PANDA: a pipeline toolbox for analyzing brain diffusion images," *Front. Hum. Neurosci.*, vol. 0, 2013.

[31] Y. Sun, Y. Chen, R. Lee, A. Bezerianos, S. L. Collinson, and K. Sim, "Disruption of brain anatomical networks in schizophrenia: A longitudinal, diffusion tensor imaging based study," *Schizophr Res*, vol. 171, no. 1-3, pp. 149–157, Mar. 2016.

[32] Y. Sun, Z. Dai, J. Li, S. L. Collinson, and K. Sim, "Modular-level alterations of structure-function coupling in schizophrenia connectome," *Hum Brain Mapp*, vol. 38, no. 4, pp. 2008–2025, Apr. 2017.

[33] Y. Sun, Y. Chen, S. L. Collinson, A. Bezerianos, and K. Sim, "Reduced hemispheric asymmetry of brain anatomical networks is linked to schizophrenia: A connectome study," *Cereb Cortex*, vol. 27, no. 1, pp. 602–615, Jan. 2017.

[34] M. Jenkinson, P. Bannister, M. Brady, and S. Smith, "Improved optimization for the robust and accurate linear registration and motion correction of brain images," *Neuroimage*, vol. 17, no. 2, pp. 825–841, Oct. 2002.

[35] S. Mori, B. J. Crain, V. P. Chacko, and P. C. van Zijl, "Three-dimensional tracking of axonal projections in the brain by magnetic resonance imaging," *Ann Neurol*, vol. 45, no. 2, pp. 265–269, Feb. 1999.

[36] G. L. Baum, D. R. Roalf, P. A. Cook, R. Ciric, A. F. Rosen, C. Xia, M. A. Elliott, K. Ruparel, R. Verma, B. Tunç *et al.*, "The impact of in-scanner head motion on structural connectivity derived from diffusion mri," *Neuroimage*, vol. 173, pp. 275–286, 2018.

[37] Z. Cui and G. Gong, "The effect of machine learning regression algorithms and sample size on individualized behavioral prediction with functional connectivity features," *Neuroimage*, vol. 178, pp. 622–637, Sep. 2018.

[38] M. Dresler, W. R. Shirer, B. N. Konrad, N. C. J. Müller, I. C. Wagner, G. Fernández, M. Czisch, and M. D. Greicius, "Mnemonic Training Reshapes Brain Networks to Support Superior Memory," *Neuron*, vol. 93, no. 5, pp. 1227–1235.e6, Mar. 2017.

[39] L. Fan et al., "The Human Brainnetome Atlas: A New Brain Atlas Based on Connectional Architecture," *Cereb Cortex*, vol. 26, no. 8, pp. 3508–3526, Aug. 2016.

[40] C. R. Buchanan, C. R. Pernet, K. J. Gorgolewski, A. J. Storkey, and M. E. Bastin, "Test-retest reliability of structural brain networks from diffusion MRI," *Neuroimage*, vol. 86, pp. 231–243, Feb. 2014.

[41] T. E. Nichols and A. P. Holmes, "Nonparametric permutation tests for functional neuroimaging: a primer with examples," *Hum Brain Mapp*, vol. 15, no. 1, pp. 1–25, Jan. 2002.

[42] S. Achard and E. Bullmore, "Efficiency and Cost of Economical Brain Functional Networks," *PLoS Comput Biol*, vol. 3, no. 2, p. e17, Feb. 2007.

[43] V. Latora and M. Marchiori, "Efficient behavior of small-world networks," *Phys Rev Lett*, vol. 87, no. 19, p. 198701, Nov. 2001.

[44] S. Kelly et al., "Widespread white matter microstructural differences in schizophrenia across 4322 individuals: results from the ENIGMA Schizophrenia DTI Working Group," *Mol Psychiatry*, vol. 23, no. 5, pp. 1261–1269, May 2018.

[45] M. Kubicki, R. McCarley, C.-F. Westin, H.-J. Park, S. Maier, R. Kikinis, F. A. Jolesz, and M. E. Shenton, "A review of diffusion tensor imaging studies in schizophrenia," *J Psychiatry Res*, vol. 41, no. 1-2, pp. 15–30, Feb. 2007.

[46] J. Chen, T. Wensing, F. Hoffstaedter, E. C. Cieslik, V. I. Müller, K. R. Patil, A. Aleman, B. Derntl, O. Gruber, R. Jardri, L. Kogler, I. E. Sommer, S. B. Eickhoff, and T. Nickl-Jockschat, "Neurobiological substrates of the positive formal thought disorder in schizophrenia revealed by seed connectome-based predictive modeling," *Neuroimage Clin*, vol. 30, p. 102666, Apr. 2021.

[47] Y. Zhang, G. Guo, and Y. Tian, "Increased temporal dynamics of intrinsic brain activity in sensory and perceptual network of schizophrenia," *Front. Psychiatry*, vol. 0, 2019.

[48] G. Foussias and G. Remington, "Negative symptoms in schizophrenia: avolition and Occam's razor," *Schizophr Bull*, vol. 36, no. 2, pp. 359–369, Mar. 2010.

[49] L. R. Skelly, V. Calhoun, S. A. Meda, J. Kim, D. H. Mathalon, and G. D. Pearlson, "Diffusion tensor imaging in schizophrenia: relationship to symptoms," *Schizophr Res*, vol. 98, no. 1-3, pp. 157–162, Jan. 2008.

[50] A. Rotarska-Jagiela, V. van de Ven, V. Oertel-Knöchel, P. J. Uhlhaas, K. Vogeley, and D. E. J. Linden, "Resting-state functional network correlates of psychotic symptoms in schizophrenia," *Schizophr Res*, vol. 117, no. 1, pp. 21–30, Mar. 2010.

[51] B.-C. Ho, N. C. Andreasen, P. Nopoulos, S. Arndt, V. Magnotta, and M. Flaum, "Progressive structural brain abnormalities and their relationship to clinical outcome: a longitudinal magnetic resonance imaging study early in schizophrenia," *Arch Gen Psychiatry*, vol. 60, no. 6, pp. 585–594, 2003.

[52] S. Liang et al., "Classification of first-episode schizophrenia using multimodal brain features: A combined structural and diffusion imaging study," *Schizophr Bull*, vol. 45, no. 3, pp. 591–599, Apr. 2019.

[53] I. Ellison-Wright and E. Bullmore, "Meta-analysis of diffusion tensor imaging studies in schizophrenia," *Schizophr Res*, vol. 108, no. 1-3, pp. 3–10, Mar. 2009.

[54] T. Asami, S. Bouix, T. J. Whitford, M. E. Shenton, D. F. Salisbury, and R. W. McCarley, "Longitudinal loss of gray matter volume in patients with first-episode schizophrenia: DARTEL automated analysis and ROI validation," *Neuroimage*, vol. 59, no. 2, pp. 986–996, Jan. 2012.

[55] B. Olabi, I. Ellison-Wright, A. M. McIntosh, S. J. Wood, E. Bullmore, and S. M. Lawrie, "Are there progressive brain changes in schizophrenia? A meta-analysis of structural magnetic resonance imaging studies," *Biol Psychiatry*, vol. 70, no. 1, pp. 88–96, Jul. 2011.
[56] P. Kochunov, D. C. Glahn, L. M. Rowland, R. L. Olvera, A. Winkler, Y.-H. Yang, H. Sampath, W. T. Carpenter, R. Duggirala, J. Curran, J. Blangero, and L. E. Hong, "Testing the hypothesis of accelerated cerebral white matter aging in schizophrenia and major depression," *Biol Psychiatry*, vol. 73, no. 5, pp. 482–491, Mar. 2013.
[57] V. L. Cropley, P. Klauser, R. K. Lenroot, J. Bruggemann, S. Sundram, C. Bousman, A. Pereira, M. A. Di Biase, T. W. Weickert, C. S. Weickert, C. Pantelis, and A. Zalesky, "Accelerated Gray and White Matter Deterioration With Age in Schizophrenia," *Am J Psychiatry*, vol. 174, no. 3, pp. 286–295, Mar. 2017.
[58] S. E. Morgan, S. R. White, E. T. Bullmore, and P. E. Vértes, "A network neuroscience approach to typical and atypical brain development," *Biol Psychiatry Cogn Neurosci Neuroimaging*, vol. 3, no. 9, pp. 754–766, Sep. 2018.
[59] K. E. Stephan, K. J. Friston, and C. D. Frith, "Dysconnection in schizophrenia: from abnormal synaptic plasticity to failures of self-monitoring," *Schizophr Bull*, vol. 35, no. 3, pp. 509–527, May 2009.
[60] D. C. Goff, P. Falkai, W. W. Fleischhacker, R. R. Girgis, R. M. Kahn, H. Uchida, J. Zhao, and J. A. Lieberman, "The Long-Term Effects of Antipsychotic Medication on Clinical Course in Schizophrenia," *Am J Psychiatry*, vol. 174, no. 9, pp. 840–849, Sep. 2017.
[61] R. Kanaan, G. Barker, M. Brammer, V. Giampietro, S. Shergill, J. Woolley, M. Picchioni, T. Toulopoulou, and P. McGuire, "White matter microstructure in schizophrenia: effects of disorder, duration and medication," *Br J Psychiatry*, vol. 194, no. 3, pp. 236–242, Mar. 2009.
[62] M. Rubinov, S. A. Knock, C. J. Stam, S. Micheloyannis, A. W. F. Harris, L. M. Williams, and M. Breakspear, "Small-world properties of nonlinear brain activity in schizophrenia," *Hum Brain Mapp*, vol. 30, no. 2, pp. 403–416, Feb. 2009.
[63] D. K. Jones, T. R. Knösche, and R. Turner, "White matter integrity, fiber count, and other fallacies: the do's and don'ts of diffusion MRI," *Neuroimage*, vol. 73, pp. 239–254, Jun. 2013.
[64] Y. Li, Y. Liu, J. Li, W. Qin, K. Li, C. Yu, and T. Jiang, "Brain anatomical network and intelligence," *PLoS Comput Biol*, vol. 5, no. 5, p. e1000395, 2009.
[65] G. Gong, Y. He, L. Concha, C. Lebel, D. W. Gross, A. C. Evans, and C. Beaulieu, "Mapping anatomical connectivity patterns of human cerebral cortex using in vivo diffusion tensor imaging tractography," *Cereb cortex*, vol. 19, no. 3, pp. 524–536, 2009.
[66] A. Zalesky, A. Fornito, L. Cocchi, L. L. Gollo, M. P. van den Heuvel, and M. Breakspear, "Connectome sensitivity or specificity: which is more important?" *Neuroimage*, vol. 142, pp. 407–420, Nov. 2016.
[67] P. Hagmann, L. Cammoun, X. Gigandet, R. Meuli, C. J. Honey, V. J. Wedeen, and O. Sporns, "Mapping the structural core of human cerebral cortex," *PLoS Biol*, vol. 6, no. 7, p. e159, 2008.
[68] C. Beaulieu, "The basis of anisotropic water diffusion in the nervous system–a technical review," *NMR Biomed*, vol. 15, no. 7-8, pp. 435–455, 2002.
[69] D. S. Tuch, V. J. Wedeen, A. M. Dale, J. S. George, and J. W. Belliveau, "Conductivity tensor mapping of the human brain using diffusion tensor MRI," *P Natl Acad Sci USA*, vol. 98, no. 20, pp. 11 697–11 701, 2001.
[70] J. Cohen, "A power primer," *Psychol Bull*, vol. 112, no. 1, pp. 155–159, Jul. 1992.
[71] G. Collin et al., "Brain functional connectivity data enhance prediction of clinical outcome in youth at risk for psychosis," *Neuroimage Clin*, vol. 26, p. 102108, Jan. 2020.